A COUPLED THERMAL AND ELECTRICAL MODEL OF A SHEET-AND-TUBE HYBRID PHOTOVOLTAIC/THERMAL (PV/T) COLLECTOR

Guarracino I., Markides C.N.* and Ekins-Daukes N.J.
*Author for correspondence
Department of Chemical Engineering,
Imperial College London,
London, SW7 2AZ,
United Kingdom,
E-mail: c.markides@imperial.ac.uk

ABSTRACT

The goal of this paper is to obtain the (pair of) efficiency curves of a hybrid PV/T collector with a sheet-and-tube design and to evaluate the effect of a non-uniform temperature distribution on the surface of the solar cell on its electrical power output. A 3-dimensional numerical model is developed to estimate the performance of such a collector. The model allows various design parameters of the PV/T to be varied so that the influence of each of these parameters can be studied on the overall system performance both at steady-state and at varying atmospheric conditions. The main parameters considered are the number of glass covers, ranging from an unglazed collector configuration to a double-glazed collector configuration, and the width-to-pipe diameter (W/D) ratio. The results show that, while the thermal efficiency increases with the additional glazing, the electrical efficiency deteriorates due to the higher temperature of the fluid and due to increased optical losses, as expected. The dynamic performance of the PV/T collector and system are also investigated. Results from the dynamic model and also from a simplified quasi-steady state model are reported. The results show that in the case of highly fluctuating incident radiation, e.g. from clouds, the quasi-steady solution can deviate by up to 20% from the dynamic solution in the evaluation of the thermal energy output in the case of low incident radiation with large fluctuations.

INTRODUCTION

The development and deployment of advanced clean energy technologies is estimated as having a potential for contributing to the reduction of CO_2 emissions of between 17% and 19% [1,2]. At the same time, declining reserves of conventional fossil fuels coupled with a growing demand for energy will exacerbate issues related to energy security and lead to an increase in energy prices. Energy security demands the implementation of sustainable and long term energy solutions. In order to promote a focus on a sustainable future, the EU has set a target of cutting greenhouse gas (GHG) emissions by 20%, reducing energy consumption by 20% and increasing market penetration of renewable technologies by 20% by 2020.

Solar heating and cooling technologies, as well as solar electricity generation, can play an important role in realising targets in energy security, economic development and climate change mitigation. Low temperature solar-thermal technologies based on flat-plate or evacuated collectors are already relatively mature and can replace electricity or gas consumption for hot water provision and space heating. Solar cooling technologies can reduce the electrical-grid load at times of peak cooling demand by replacing conventional electrically driven compression chillers for air conditioning. Further, photovoltaic (PV) collectors can convert sunlight directly into electricity.

Sunlight can be converted into heat and electricity simultaneously in an integrated photovoltaic/thermal hybrid solar collector (PV/T), which is a combination of a PV and a solr-thermal system. Monocrystalline c-Si cells, the type considered in this study, can only convert radiation with wavelengths below the threshold value of 1.1 μm to electricity [3]. The greatest part of the absorbed radiation in a PV module is thus converted into heat (about 60% – 70%), increasing the temperature of the solar cell and reducing its conversion efficiency [4]. In a PV/T system this low-grade heat is collected in the thermal absorber and recovered by a fluid stream (for domestic hot water and for heating or cooling in domestic and commercial applications).

A PV/T system aims to improve the overall conversion efficiency of the PV panel by cooling the solar cells. The performance of a PV module is strongly dependent on its operating temperature. The temperature gradients on the surface of a PV/T collector significantly affect its electrical efficiency since solar cells operating at higher temperatures generate less power, and therefore a significant challenge in the design of a PV/T collector is in obtaining a uniform temperature distribution over the modules. A sheet-and-tube collector is associated with a non-uniform temperature on its top surface during operation. The prediction of this temperature distribution is therefore of crucial importance when selecting the best design and evaluating the thermal and the electrical yield of the associated PV/T system.

In this paper, a 3-D dynamic numerical model is developed and used to evaluate the thermal and electrical performance of a hybrid PV/T sheet-and-tube collector. It solves the energy balance by taking into account the convective and radiative losses from the top surface of the collector and the optical losses due to reflection. The electrical model estimates the operating current and voltage of each individual cell and of the entire module by considering the non-uniform temperature distribution.

This work aims to characterize in detail the electrical and thermal efficiencies, and the current voltage (I-V) curve of the

PV/T collector taking into account the temperature variation along the flow direction and between tubes. The numerical approach is based on the previous work of authors such as in Refs. [4-5]. The model presented in this paper can generate results for the hourly performance analysis under varying operating condition and can also provide information on the transient response of the collector when it is operating under varying atmospheric conditions.

NOMENCLATURE

c	[J/kgK]	Specific heat capacity
D	[m]	Tube diameter
E	[W]	Electrical power, energy
f	[-]	Fraction
h	[W/m^{2}K]	Convective heat transfer coefficient
I	[A]	Current
J	[A/m^2]	Current density
k	[W/mK]	Thermal conductivity
m	[kg/s]	Mass flow rate
Nu	[-]	Nusselt number
Pr	[-]	Prandtl number
Q	[W]	Energy flux
R	[m^{2}K/W]	Interfacial thermal resistance
Ra	[-]	Rayleigh number
Re	[-]	Reynolds number
T	[K]	Temperature
V	[V]	Voltage
W	[m]	Tube spacing
x	[m]	Cartesian axis direction
y	[m]	Cartesian axis direction
z	[m]	Cartesian axis direction

Special characters

α	[-]	Absorptance
β	[K^{-1}]	Temperature coefficient
ε	[-]	Surface emissivity, heat exchanger effectiveness
η	[-]	Efficiency
τ	[-]	Transmittance

Subscripts

A	Thermal absorber
a	Ambient
CD	Conductive
ci, co	Collector inlet, outlet
E	Electrical energy, power
f	Fluid
free	Free convection
g	Glass, band gap
gap	Air gap
H	Hydraulic
h	Heat exchanger
HW	Domestic hot water
l	Load
loss	Energy losses
m	Mains water
p	Pipe
PV	Solar cell
SC	Short circuit
t	Tank
w	Wind

MODELLING METHODOLOGY

The numerical model evaluates the electrical and thermal efficiencies of an unglazed, glazed and doubly glazed PV/T collectors. Each collector is composed of three basic layers: glass cover(s), PV module and thermal absorber (Figure 1). The PV module comprises c-Si solar cells placed in between a top transparent surface, an encapsulant and a rear layer. The encapsulant is ethyl vinyl acetate (EVA) in most modules, and the rear layer is Tedlar, while the transparent top surface consists of low iron glass [6].

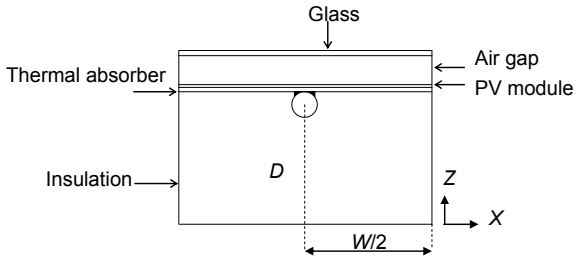

Figure 1 Cross section *z*-*x* of a single glazed PV/T module having a pipe diameter D and a distance between pipes W

The model developed here is based on the assumptions of:

1. Negligible edge thermal losses.
2. Constant thermal and optical properties of all materials.
3. A maximum temperature existing between adjacent pipes.

In addition, for a sheet-and-tube collector, the water flow rate and fluid temperature at the inlet of each parallel tube can be taken as being the same [7]. Assuming a uniform incident solar radiation G, wind speed V_w and ambient temperature T_a, the temperature distribution between two adjacent pipes is then symmetric.

The energy balance equation is solved numerically along the water-flow direction y and the transverse direction x, where each layer is discretized into N_x and N_y number of nodes. Each layer is assumed to have uniform thermophysical properties in the z-direction. The solution of the energy balance is a 2-D temperature distribution over each layer of the PV/T module. This distribution is used to evaluate the *I-V* curve of the PV module by neglecting the electrical resistance between the solar cells.

The 3-D model allows for the evaluation of the instantaneous electrical and thermal efficiency and of the efficiency curves of the PV/T module. The thermal efficiency curve of the PV/T module can then be plotted against the reduced temperature $T^* = (T_{ci} - T_a)/G$. After evaluating the temperature distribution on the solar cells, an electrical model calculates the *I-V* curve and the maximum power point under varying operating conditions.

The dynamic numerical model of the PV/T module is integrated within a wider dynamic model of a system for the provision of domestic hot water. This is a simplified model, as represented in Figure 2, consisting of a storage tank, the PV/T collector, a circulating pump, a bypass branch which allows for the recirculation of the water in the solar collector until the fluid reaches the desired temperature, and a heat exchanger.

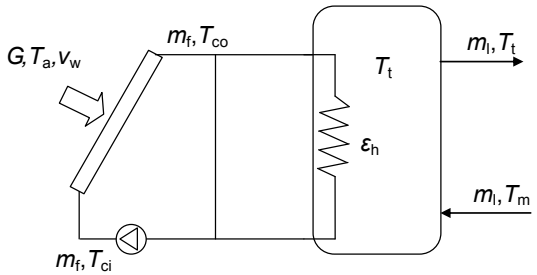

Figure 2 Schematic diagram of a PV/T system for the provision of domestic hot water

The thermal and electrical energy outputs of the PV/T system are evaluated for a 3-bedroom terraced house in the UK. This system was previously studied in Ref. [8] and so the input data for the consumption of domestic hot water and electrical power are taken from this work and used for the simulation of the PV/T system with the three collector-array designs of interest, i.e.: single glazed, unglazed and double-glazed.

PV/T unit, thermal model equations

The 3-D dynamic thermal model solves the energy balance equations at each layer of the PV/T module. This section reports the set of equations describing the thermal behaviour of the single-glazed PV/T module. The fundamental equations of the dynamic model of the collector are presented in Equations (1) to (3). The same equations can be used for the double-glazed and unglazed PV/T collector configurations, and also for the conventional thermal collector.

$$\rho_g c_g \delta_g \frac{\partial T_g}{\partial t} = \delta_g k_g \frac{\partial^2 T_g}{\partial x^2} + \delta_g k_g \frac{\partial^2 T_g}{\partial y^2} - \varepsilon_g \sigma (T_g^4 - T_{sky}^4) - h_{top}(T_g - T_a) + \sigma \left(\frac{1}{1/\varepsilon_g + 1/\varepsilon_{PV} - 1} \right) (T_{PV}^4 - T_g^4) + 1/R_{gap}(T_{PV} - T_g) + \alpha_g G \quad (1)$$

$$\rho_{PV} c_{PV} \delta_{PV} \frac{\partial T_{PV}}{\partial t} = \delta_{PV} k_{PV} \frac{\partial^2 T_{PV}}{\partial x^2} + \delta_{PV} k_{PV} \frac{\partial^2 T_{PV}}{\partial y^2} + \overline{\tau\alpha}_{PV} G - \overline{\tau\alpha}_{PV} G \eta_{el} - \sigma \left(\frac{1}{1/\varepsilon_g + 1/\varepsilon_{PV} - 1} \right) (T_{PV}^4 - T_g^4) - 1/R_{gap}(T_{PV} - T_g) - 1/R_{CD}(T_{PV} - T_A) \quad (2)$$

$$\rho_A c_A \delta_A \frac{\partial T_A}{\partial t} = \delta_A k_A \frac{\partial^2 T_A}{\partial x^2} + \delta_A k_A \frac{\partial^2 T_A}{\partial y^2} + 1/R_{CD}(T_{PV} - T_A) - 1/R_f(T_A - T_f) - 1/R_{loss}(T_A - T_a) \quad (3)$$

Equations (1) to (3) are energy-balance equations applied to the glass, solar cell and absorber plate, respectively. The heat transfer coefficient h_{top} in Equation (1) is the convective heat transfer coefficient, which takes into account the free convection and the forced convection in the case of wind, as:

$$h_{top} = \sqrt[3]{h_w^3 + h_{free}^3} \ . \quad (4)$$

A review of various correlations for h_w is given in Ref. [9]. In in most of these correlations h_w is a linear function of the wind velocity. In addition, h_{free} is a function of the Rayleigh (Ra) number evaluated on the plate top-surface at a mid-temperature between the ambient and the glass as given in Ref. [10].

The thermal resistance R_{gap} between the glass and the solar cell in Equations (1) and (2) accounts for convection in the air gap and conduction at the top layers of the solar cell (top transparent layer and encapsulant). The convective heat transfer coefficient h_{gap} ($h_{gap} = Nu_{gap} k_{air}/\delta_{gap}$) in the enclosed space is [11]:

$$h_{gap} = \frac{k_{air}}{\delta_{gap}} 1 + 1.44 \left(1 - \frac{1708}{Ra \cos\gamma} \right)^* \left(1 - \frac{1708(\sin 1.8\gamma)^{1.6}}{Ra \cos\gamma} \right) + \left[\left(\frac{Ra \cos\gamma}{5830} \right)^{1/3} - 1 \right]^* \quad (5)$$

In this equation:

1. The dotted brackets go to zero when they are negative.
2. Ra is the Rayleigh number ($Ra = g\beta\rho c/k\mu\Delta T\delta_{gap}^3$).
3. γ is the tilt angle of the collector to the horizontal.
4. k_{air} is the thermal conductivity of the fluid evaluated at the average temperature $T_H - \Delta T/2$, where T_H is the temperature of the hot surface and ΔT the temperature difference between the two surfaces.
5. δ_{gap} is the gap between the two layers.

The electrical efficiency η_{el} in Equation (2) is a linear function of the temperature of the solar cell [5]:

$$\eta_{el} = \eta_{ref} [1 - \beta (T - T_{ref})] \ . \quad (6)$$

The temperature coefficient β in Equation (6) gives the efficiency drop when the operating temperature of the solar cell T_{PV} is higher than the standard operating temperature (T_{ref}).

The transmission-absorption coefficient $\overline{\tau\alpha}$ for a glazed system is calculated with the ray tracing technique as reported in Refs. [12,13]. For a single-glazed system, as in Equation (2), $\overline{\tau\alpha}$ is:

$$\overline{\tau\alpha} = \frac{\tau_g \alpha_{PV}}{(1 - \alpha_{PV})^2} \ . \quad (7)$$

The thermal resistance R_f in Equation (3) takes into account the thermal losses associated with the conduction through the pipe wall and the convective heat transfer in the fluid. In the case of forced circulation for fully developed flow, the convective heat transfer coefficient h_f is [10]:

$$h_f = 4.36 \frac{k_f}{D_H} \quad \text{for } Re < 2300 \ ; \quad (8)$$

$$h_f = \frac{k_f}{D_H} 0.023 Re_f^{0.8} Pr_f^{0.4} \quad \text{for } Re > 2300 \ . \quad (9)$$

The thermal resistance R_{loss} in Equation (3) takes into account the conduction through the insulation and the free convection to the ambient.

Finally, the boundary conditions required to solve the energy balance are given in Equations (10) to (12).

$$T_{f-in} = T_{ci} \quad (10)$$

$$\left. \frac{\partial T}{\partial x} \right|_{x=0, W/2} = 0 \quad (11)$$

$$\left. \frac{\partial T}{\partial y} \right|_{y=0, L} = 0 \quad (12)$$

PV/T unit, electrical model equations

The temperature on the solar cell resulting from the thermal energy balance has a non-uniform distribution over the x-y plane. The I-V curve of the PV module calculated considering the non-uniform temperature distribution by solving a simplified electrical model of the PV module, which neglects the electrical resistances. The current density generated at a fixed temperature and irradiation is calculated as [14]:

$$J = J_{SC} - CT^3 \exp\left[\frac{-E_g(T)}{KT} \right] \exp\left[\frac{V}{KT} \right] , \quad (13)$$

where $C = 5688.5$ A/m^{2}K^3 and K is the Boltzmann constant scaled by the electronic charge. The band-gap energy in Equation (13) is calculated as a function of the operating temperature of the solar cell and of the band-gap energy at 0 K as [14]:

$$E_g(T) = E_g(0) - \frac{aT^2}{T + b} \ . \quad (14)$$

Equations (13) and (14) are used to calculate the *I-V* curve of each solar cell operating at non uniform temperature. The *I-V* characteristic of the PV/T module is calculated by assuming that the solar cells are connected in series.

System model

The performance of a PV/T system is evaluated in terms of its thermal output (provision of domestic hot water) and electrical energy output. The inlet fluid temperature of the collector is the result of the energy balance at the storage tank, by accounting for the demand of hot water, the heat losses at the storage tank and the efficiency of the heat exchanger as expressed in Equation (15). The storage tank is assumed to be fully mixed and the temperature at the outlet of the heat exchanger immersed in the storage tank is given in Equation (16), while the energy for supplying domestic hot water is given in Equation (17).

$$M_t c_t \frac{dT_t}{dt} = Q_{coll} - Q_l - Q_{loss} \quad (15)$$

$$Q_{coll} = m_f c_f \varepsilon_H (T_{co} - T_t) \quad (16)$$

$$Q_l = m_l c_l (T_m - T_t) \quad (17)$$

The flow from the PV/T collector is allowed to circulate in the heat exchanger only if the collector outlet fluid temperature T_{co} is greater than the water temperature in the storage tank T_t. A bypass branch allows the recirculation of the fluid in the PV/T collector until it reaches a temperature greater than that of the water in tank.

PRELIMINARY RESULTS

The design parameters investigated are the width-to-pipe diameter (*W/D*) ratio and the influence of glazing. The thermal model allows for the prediction of the temperature distribution on the solar cell, which is then used as the input to the electrical model. The temperature on the solar cell has a maximum between two adjacent pipes and increases in the flow direction as the coolant collects thermal energy from the absorber, as shown in Figure 3. Both the thermal and electrical efficiencies (and thermal and electrical power outputs) are reduced as the spacing between two pipes is increased (high *W/D* ratio). The results are reported for the single glazed configuration in Figure 4. An increase in the width-to-pipe diameter ratio leads to an increased temperature at the top layer of the collector, and thus an increase in the convective and radiative thermal losses Q_{loss} to the environment.

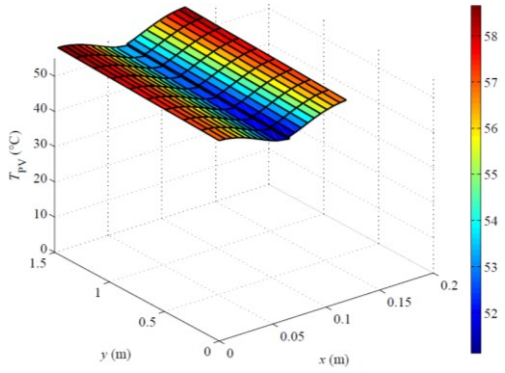

Figure 3 Temperature distribution T_{PV} over the solar cell between two adjacent pipes at operating conditions with G = 1000 W/m^2, T_{ci} = 25 °C and T_a = 25 °C

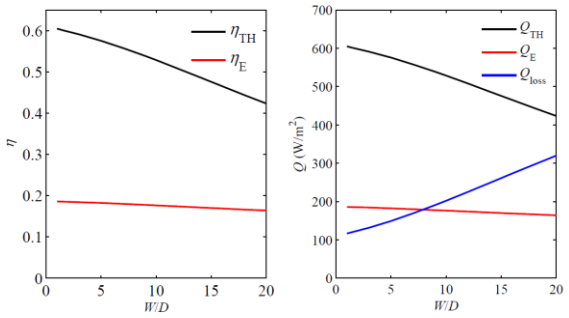

Figure 4 Thermal and electrical efficiencies η (left) and energy outputs Q (right) of the PV/T single glazed collector as function of the ratio *W/D*

The thermal efficiency can be improved by glazing, owing to the reduction in the convective losses. Figure 5 shows that a double-glazed collector delivers a higher thermal efficiency compared to a single-glazed or unglazed collector, however, the electrical efficiency deteriorates due to the optical losses which account for 14% of the reflected radiation for the double glazed, 12% for the single glazed and 10% for the unglazed collector.

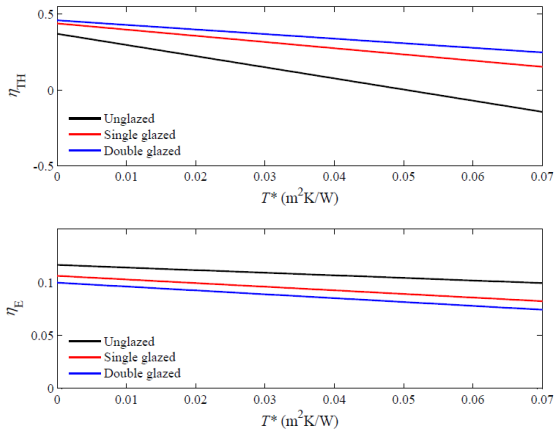

Figure 5 Thermal efficiency η_{TH} and electrical efficiency η_{EL} of the PV/T collector for the three configurations as function of the reduced temperature *T**

Figure 6 shows the *I-V* curve of the single-glazed PV/T collector at a uniform temperature of 25 °C and at the non-uniform operating temperature calculated with the thermal model. This collector is made of 6 parallel pipes and 60 solar cells connected in series, with an aperture area of 62 m^2 [8]. According to the electrical specifications given in Ref. [8] the power output is 250 W and the open-circuit voltage is 36.9 V. The open-circuit voltage V_{OC} drops from 36.9 V to 32.7 V, when the PV module operates at standard conditions, with a loss in power output of 34 W equal to 13% of the maximum power output at standard operating conditions.

The variation of the open-circuit voltage V_{OC} of this module with the incident solar radiation G is reported in Figure 7. The open-circuit voltage displays a maximum value for an incident solar radiation between G = 300 W/m^2 and G = 600 W/m^2, while the maximum power output always increases with the incident solar radiation since the current generated increases with the solar radiation, as expected.

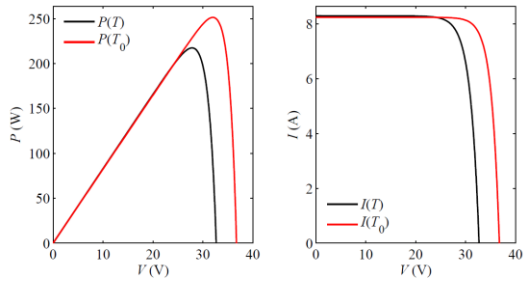

Figure 6 *I-V* curve of the PV/T module at the reference temperature T_0 and at operating temperature T

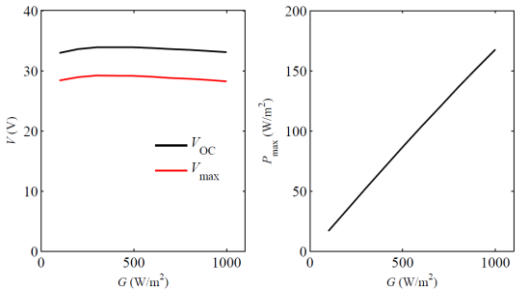

Figure 7 Variation of the open circuit voltage V_{oc}, voltage at the maximum power and maximum power output with the incident solar radiation

The behaviour of the PV/T module can be simulated under transient conditions of solar radiation, ambient temperature and wind speed. A study was performed in which the inlet temperature of the water was kept constant whilst these quantities were allowed to vary. The results of a step variation of solar radiation for the three studied configurations of the PV/T collector are reported in Figure 8. The unglazed collector responds faster than the glazed ones, and the double-glazed configuration has the slowest response time.

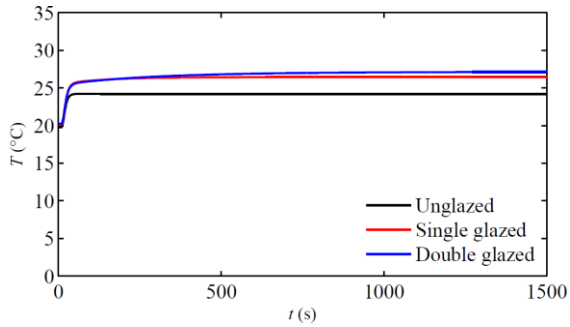

Figure 8 Fluid outlet temperature of the PV/T collector as response to a step variation in the incident solar radiation G from 50 W/m^2 to 1000 W/m^2

Furthermore, the dynamic response of the three PV/T collectors has been investigated for a case of highly time-fluctuating incident solar radiation. The data of solar radiation, ambient temperature and wind speed were collected in London with a resolution of 1 min. The behaviour of the single-glazed PV/T collector was simulated at the conditions of constant flow rate and inlet fluid temperature of 20 °C, while the ambient conditions were allowed to vary. The variation of the fluid temperature ΔT for a single-glazed collector is reported in Figure 9 for two time-steps of 5 s and 60 s, along with the quasi-steady solution. A time-step Δt of 5 s or smaller was found to be sufficient to ensure the solution is non-dependent on the time-step chosen to run the simulation.

The average value of ΔT obtained with a Δt of 60 s deviates by 49% from the solution having a Δt of 5 s, while the quasi-steady solution deviates by 20% (mainly due to time-shifting). These values are obtained for a case study of low incident radiation and small ΔT across the collector. The error on the collector outlet fluid temperature for the same scenario is 0.060% with Δt of 60 s and 0.045% for the quasi-steady solution.

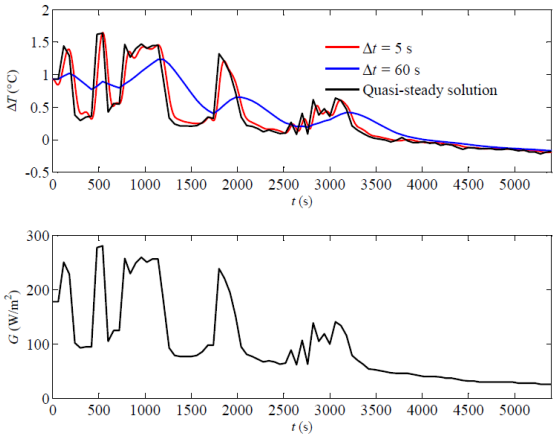

Figure 9 Variation of the fluid temperature ΔT in a single glazed collector under a highly varying solar radiation G. The solution of the dynamic model is reported for a time-step Δt of 5 s and 60 s together with the quasi-steady solution

Proceeding further, the yearly performance of the PV/T system can be evaluated based on the above solutions, by considering the daily demand profiles of the hot water and electricity. A repetitive average daily load profile of domestic hot water demand is considered this simulation, while the electricity demand profile is taken from a model developed by the Centre for Renewable Energy Systems Technology (CREST) as described in Refs. [8,15].

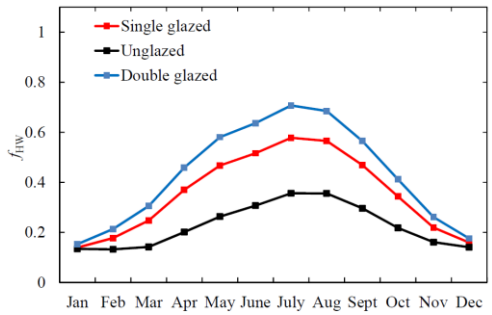

Figure 10 Fraction of the demand of hot water f_{HW} generated by the PV/T system for the three configurations

Figures 10 and 11 show the fraction of the monthly thermal energy and electricity provided by the PV/T system for the three configurations of unglazed, single-glazed and double-glazed collector. As expected, a system with an array of double

glazed collectors would cover a larger fraction of thermal energy demand but a lower fraction of electrical energy demand. During periods of high-irradiation conditions, the electricity demand is fully covered by the PV/T system, while a backup system for providing hot water is required all year long.

Furthermore, Figures 12 and 13 show the daily generation of electricity in July and of hot water in July and December. It can be observed that the PV/T system can provide part of the demand for thermal energy in December, when the availability of solar energy is the lowest of the year, thanks to the thermal energy storage capability provided by the hot-water tank.

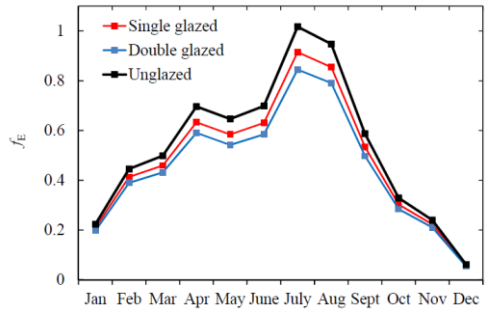

Figure 11 Fraction of the demand of electricity f_{EL} generated by the PV/T system for the three configurations

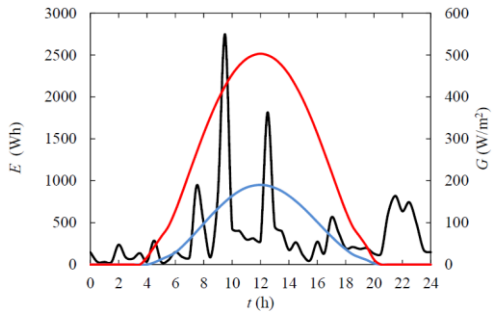

Figure 12 Electricity *E* generated by the PV/T single glazed system (blue line) compared with the demand of electricity (black line) for a day in July at the incident solar radiation *G* (red line)

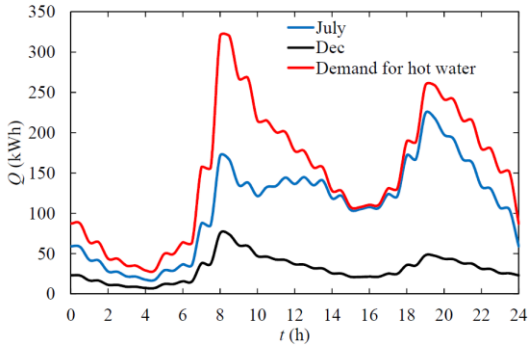

Figure 13 Thermal energy provided by the PV/T single glazed system in July and December (blue and red line) compared with the demand of domestic hot water (black line)

CONCLUSION

A 3-D dynamic numerical model is developed that allows for the estimation of PV/T collector performance over a wide range of operating conditions by predicting both its thermal and electrical outputs and efficiencies. Results of parametric analyses based on this model can be used to identify the effects of important design and operating parameters, leading to improved designs for chosen applications. The thermal and electrical efficiencies can be improved by reducing the width-to-diameter ratio *W*/*D*. Thus, alternative designs which reduce the spacing between the channels for circulating fluid are worth investigating. Adding additional glazing improves the thermal efficiency and increases the fraction of the thermal energy provided, but the electrical efficiency and the electricity generated are reduced due to the optical losses. A quasi-steady state solution of a dynamic problem can also be adopted, resulting in an error on the prediction of the performance of the collector. When the radiation varies sharply and rapidly with time the quasi-steady solution has an error on the operating temperature of the collector up to 20%, which is mainly due to time shifting. Also adopting a large time-step (60 s in this simulation) determines a solution with 49% error.

REFERENCES

[1] International Energy Agency, Energy Technology Perspectives 2010, Scenarios and Strategies to 2050, 2010

[2] Markides, C.N., The role of pumped and waste heat technologies in a high-efficiency sustainable energy future for the UK, *Applied Thermal Engineering*, Vol. 53, 2013, pp. 197-209

[3] Santbergen, R., and van Zolingen, R.C., The absorption factor of crystalline silicon PV cells: a numerical and experimental study, *Solar Energy Materials and Solar Cells*, Vol. 92, 2008, pp. 432-444

[4] Dupeyrat, P., Menezo, C., and Fortuin, S., Study of the thermal and electrical performances of PVT solar hot water system, *Energy and Buildings*, Vol. 68, 2014, pp. 751-755

[5] Zondag, H.A., de Vries, D.W., van Helden, W.G.J., van Zolingen, R.J.C., and van Steenhoven, A.A., The thermal and electrical yield of a PV-thermal collector, *Solar Energy*, Vol. 72, 2002, pp. 113-128

[6] Tiwari, A., and Sodha, M. S., Performance evaluation of solar PV/T system: An experimental validation, *Solar Energy*, Vol. 80, 2006, pp. 751-759

[7] Chow, T.T., Performance analysis of photovoltaic-thermal collector by explicit dynamic model, *Solar Energy*, Vol. 75, 200, pp. 143-152

[8] Herrando, M., Markides, C.N., and Hellgardt, K., A UK-based assessment of hybrid PV and solar-thermal systems for domestic heating and power: System performance, *Applied Energy,* Vol. 122, 2014, pp. 288-309

[9] Armstrong, S., and Hurley, W. G., A thermal model for photovoltaic panels under varying atmospheric conditions, *Applied Thermal Engineering*, Vol. 30, 2010, pp. 1488-1495

[10] Incropera, F.P., Fundamentals of heat and mass transfer, *Wiley*, 2011.

[11] Buchberg, H., Catton, I., and Edwards, D.K., Natural convection in enclosed spaces — A review of application to solar energy collection, *Journal of Heat Transfer*, Vol. 98, 1976, pp. 182-188

[12] Duffie, J.A., and Beckman, W.A., Solar engineering of thermal processes, *Wiley*, New York, 1980.

[13] Viskanta, R., Siebers, D.L., and Taylor, R.P., Radiation characteristics of multiple-plate glass systems, *International Journal of Heat and Mass Transfer*, Vol. 21, 1978, pp. 815-818

[14] Varshni, Y.P., Temperature dependence of the energy gap in semiconductors, *Physica*, Vol. 34, 1967, pp. 149-154.

[15] Richardson, I., Thomson, M., Infield, D., and Clifford, C., Domestic electricity use: A high-resolution energy demand model. *Energy Buildings*, Vol. 42, 2010, pp. 1878-1887